

65 nm feature sizes using visible wavelength 3-D multiphoton lithography

Wojciech Haske[†], Vincent W. Chen[†], Joel M. Hales, Wenting Dong, Stephen Barlow, Seth R. Marder, Joseph W. Perry*

[†]These authors contributed equally to this work

School of Chemistry and Biochemistry and Center for Organic Photonics and Electronics,
Georgia Institute of Technology, Atlanta, GA 30332-0400
joe.perry@gatech.edu

Abstract: Nanoscale features as small as 65 ± 5 nm have been formed reproducibly by using 520 nm femtosecond pulsed excitation of a 4,4'-bis(di-*n*-butylamino)biphenyl chromophore to initiate crosslinking in a triacrylate blend. Dosimetry studies of the photoinduced polymerization were performed on chromophores with sizable two-photon absorption cross-sections at 520 and 730 nm. These studies show that sub-diffraction limited line widths are obtained in both cases with the lines written at 520 nm being smaller. Three-dimensional multiphoton lithography at 520 nm has been used to fabricate polymeric woodpile photonic crystal structures that show stop bands in the near-infrared spectral region.

©2007 Optical Society of America

OCIS codes: (220.3740) Lithography; (190.4180) Multiphoton processes; (350.3450) Laser-induced chemistry; (999.9999) Photonic bandgap materials; (999.9999) Nanofabrication

References and links

1. B. H. Cumpston, S. P. Ananthavel, S. Barlow, D. L. Dyer, J. E. Ehrlich, L. L. Erskine, A. A. Heikal, S. M. Kuebler, I. Y. S. Lee, D. McCord-Maughon, J. Qin, H. Rockel, M. Rumi, X.-L. Wu, S. R. Marder, J. W. Perry, "Two-photon polymerization initiators for three-dimensional optical data storage and microfabrication," *Nature* **398**, 51-54 (1999).
2. W. Zhou, S. M. Kuebler, K. L. Braun, T. Yu, J. K. Cammack, C. K. Ober, J. W. Perry, S. R. Marder, "An Efficient Two-Photon-Generated Photoacid Applied to Positive-Tone 3D Microfabrication," *Science* **296**, 1106-1109 (2002).
3. J. Serbin, A. Egbert, A. Ostendorf, B. N. Chichkov, R. Houbertz, G. Domann, J. Schulz, C. Cronauer, L. Fröhlich, M. Popall, "Femtosecond laser-induced two-photon polymerization of inorganic-organic hybrid materials for applications in photonics," *Opt. Lett.* **28**, 301-303 (2003).
4. F. Stellacci, C. A. Bauer, T. Meyer-Friedrichsen, W. Wenseleers, V. Alain, S. M. Kuebler, S. J. K. Pond, Y. Zhang, S. R. Marder, J. W. Perry, "Laser and Electron-Beam Induced Growth of Nanoparticles for 2D and 3D Metal Patterning," *Adv. Mater.* **14**, 194-198 (2002).
5. M. Rumi, J. E. Ehrlich, A. A. Heikal, J. W. Perry, S. Barlow, Z. Hu, D. McCord-Maughon, T. C. Parker, H. Rockel, S. Thayumanavan, S. R. Marder, D. Beljonne, J. L. Bredas, "Structure-Property Relationships for Two-Photon Absorbing Chromophores: Bis-Donor Diphenylpolyene and Bis(styryl)benzene Derivatives," *J. Am. Chem. Soc.* **122**, 9500-9510 (2000).
6. S. M. Kuebler, M. Rumi, T. Watanabe, K. Braun, B. H. Cumpston, A. A. Heikal, L. L. Erskine, S. Thayumanavan, S. Barlow, S. R. Marder, J. W. Perry, "Optimizing Two-Photon Initiators and Exposure Conditions for Three-Dimensional Lithographic Microfabrication," *J. Photopolym. Sci. Technol.* **14**, 657-668 (2001).
7. M. Deubel, G. Von Freymann, M. Wegener, S. Pereira, K. Busch, C. M. Soukoulis, "Direct laser writing of three-dimensional photonic-crystal templates for telecommunications," *Nat. Mater.* **3**, 444-447 (2004).
8. P. Galajda, and P. Ormos, "Complex micromachines produced and driven by light," *Appl. Phys. Lett.* **78**, 249-251 (2001).
9. J. D. Pitts, P. J. Campagnola, G. A. Epling, S. L. Goodman, "Submicron multiphoton free-form fabrication of proteins and polymers: studies of reaction efficiencies and applications in sustained release," *Macromolecules* **33**, 1514-1523 (2000).
10. S. Kawata, H.-B. Sun, T. Tanaka, K. Takada, "Finer features for functional microdevices," *Nature* **412**, 697-698 (2001).
11. K. Takada, H.-B. Sun, S. Kawata, "Improved spatial resolution and surface roughness in photopolymerizationbased laser nanowriting," *Appl. Phys. Lett.* **86**, 071122-071121 (2005).

12. K. Takada, H.-B. Sun, S. Kawata, "The study on spatial resolution in two-photon induced polymerization," Proc. SPIE **6110**, 61100A-1–61100A-7 (2006).
 13. S. Juodkazis, V. Mizeikis, K. K. Seet, M. Miwa, H. Misawa, "Two-photon lithography of nanorods in SU-8 photoresist," Nanotechnology **16**, 846-849 (2005).
 14. M. Straub, and M. Gu, "Near-infrared photonic crystals with higher-order bandgaps generated by two-photon photopolymerization," Opt. Lett. **27**, 1824-1826 (2002).
 15. G. Lemercier, J.-C. Mulatier, C. Martineau, R. Anemian, C. Andraud, I. Wang, O. Stephan, N. Amari, P. Baldeck, "Two-photon absorption: from optical power limiting to 3D microfabrication," C. R. Chimie **8**, 1308-1316 (2005).
 16. M. Rumi, School of Chemistry and Biochemistry and Center for Organic Photonics and Electronics, Georgia Institute of Technology, Atlanta, Georgia 30332-0400 (unpublished results, 2006).
 17. A. S. Kewitsch, A. Yariv, "Self-focusing and self-trapping of optical beams upon photopolymerization," Opt. Lett. **21**, 24-26 (1996).
 18. S. M. Kuebler, B. H. Cumpston, S. Ananthavel, S. Barlow, J. E. Ehrlich, L. L. Erskine, A. A. Heikal, D. McCord-Maughon, J. Qin, H. Rockel, M. Rumi, S. R. Marder, J. W. Perry, "Three-dimensional microfabrication using two-photon activated chemistry," Proc. SPIE **3937**, 97-105 (2000).
 19. S. Y. Lin, J. G. Fleming, D. L. Hetherington, B. K. Smith, R. Biswas, K. M. Ho, M. M. Sigalas, W. Zubrzycki, S. R. Kurtz, J. Bur, "A three-dimensional photonic crystal operating at infrared wavelengths," Nature **394**, 251-253 (1998).
-

1. Introduction

Laser-excited two-photon or multiphoton photochemistry allows for the patterning of materials with true three-dimensional (3D) spatial resolution and provides a method for the direct laser writing of arbitrary three-dimensional structures. 3D multiphoton lithography (MPL) has matured significantly as a 3D fabrication technology since its inception. Significant progress has been made in the development of photoactive materials systems for MPL, including negative [1] and positive [2] tone polymer systems, inorganic-organic hybrid materials [3], and metal nanocomposites [4], which provide means for 3D fabrication in a variety of material types. The development of chromophores with large two-photon absorption (2PA) cross-sections [5] and sizable quantum yields for generation of reactive species has resulted in efficient materials, which can be patterned with low-power femtosecond lasers [6]. 3D microstructures and devices fabricated using MPL include photonic crystals [7], mechanical structures with moveable [8] or interlocking parts [6], microchannel and microfluidic devices [2], and biocompatible templates [9].

There is considerable interest in the potential for the fabrication of 3D structures with nanoscale resolution using MPL. It has been shown that feature widths below the diffraction limit of one-photon processes can be obtained with MPL. Kuebler *et al.* [6] have reported on the fabrication of woodpile structures with line widths of 200 nm using 730 nm laser excitation [6]. Features with 120 nm [10] and later 100 nm resolution obtained through introduction of radical quenchers [11] have been reported by Kawata *et al.* and narrower features have been obtained through the use of controlled post-fabrication shrinkage [12]. Misawa *et al.* [13] have reported very narrow widths, which have been attributed to exposure based "baking" of features; however, the reproducibility of these features was limited. Although sub-diffraction-limited transverse feature sizes can be obtained, it is clear that the attainable resolution is controlled by the width of the nonlinear dose function at or above the dose threshold of the material and that this width is fundamentally related to the wavelength of the excitation radiation. While there are a few reports of MPL using visible excitation [14, 15], the initiating systems used were typically un-optimized and the feature sizes produced were not exceedingly small (> 200 nm). Accordingly, we have investigated the resolution of MPL in a radical-initiated, crosslinkable acrylate resin system using a "donor- π -donor" chromophore designed for effective excitation at a shorter wavelength than has been typically utilized, and for good solubility in the resin.

In this paper, we report on the reliable fabrication of nanoscale polymeric features with a width as small as 65 nm using 520 nm femtosecond pulse excitation. We present studies of

the scan speed and power dependence of the feature widths for 520 and 730 nm excitation to determine the dose dependence of the widths, which provide insight into the order of the excitation process. We also demonstrate the fabrication of woodpile-type face-centered tetragonal photonic crystal (PC) structures with 65 nm line widths and lateral periodicity of 500 nm. These photonic bandgap (PBG) structures were found to have fundamental stop bands in the 700 – 1000 nm spectral region.

2. Experimental details

2.1 Materials

The photosensitive resin used for the MPL consisted of a 50:50 wt% blend of triacrylate monomers (Sartomer SR9008 and SR368, used as received) along with 0.1 wt% photoinitiator consisting of either 4,4'-bis(di-*n*-butylamino)biphenyl (DABP) or *E,E*-1,4-bis[4-(di-*n*-butylamino)styryl]-2,5-dimethoxybenzene (DABS). The chemical structures of the photoinitiators are shown in Fig. 1. DABS has been shown to be an extremely effective two-photon absorbing radical photoinitiator [1] that exhibits a maximum 2PA cross-section at 730 nm of 900 GM ($1 \text{ GM} = 1 \times 10^{-50} \text{ cm}^4 \text{ sec photon}^{-1}$) [5]. DABP is a “donor- π -donor” chromophore with shorter conjugation length than DABS that has been shown to possess a peak 2PA cross-section (~200 GM) at an excitation wavelength of 520 nm [16]. It should be noted that for resin systems that excluded both of these photoinitiators, no photoinduced polymerization was observed.

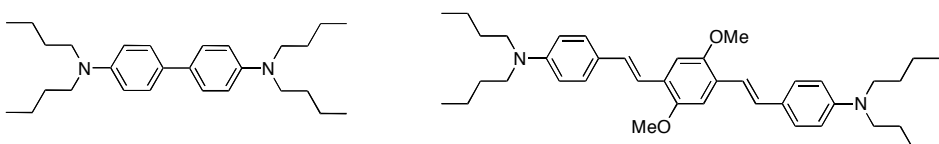


Fig. 1. Molecular structures of photoinitiators used in this work, DABP (left) and DABS (right).

The liquid resin was contained in a sample cell consisting of a microscope slide and a coverslip substrate separated by a 100 μm thick Teflon ring spacer. The coverslip was treated with an adhesion promoter (trimethoxy[2-(7-oxabicyclo-[4.1.0]hept-3-yl)ethyl]silane). Following exposure, the sample was rinsed twice in methanol for a total of 15 minutes to remove the unexposed resin. The refractive indices of the resin system were determined using an Abbe refractometer (Milton Roy) at wavelengths close to those used for excitation.

2.2 Dose-dependent photoinduced polymerization studies

Two different laser systems were used during the course of this work. The first system consisted of a tunable optical parametric amplifier (OPA-800CF, Spectra-Physics) pumped via a Ti:Sapphire regenerative amplifier (Spitfire, Spectra-Physics) providing ~100 fs pulses at a repetition rate of 1 kHz and tunable from 460 nm to 2100 nm. This system was employed for feature writing in the dose-dependent studies as well as for fabrication of the PCs and spectral characterization of the finished PBG structures. The second system was a Ti:Sapphire oscillator (Tsunami, Spectra-Physics) operating at 730 nm and a repetition rate of 82 MHz with 80 fs pulses. This system was used for the fabrication of support structures (see below) in the dose-dependent studies.

A dose-dependent photo-induced polymerization study was carried out with both DABP and DABS to compare the feature sizes of the structures created using different excitation wavelengths. The wavelengths were chosen to coincide with the peak of the two-photon cross-section for each of the dyes, i.e. 730 nm for DABS and 520 nm for DABP. The two excitation beams were delivered collinearly into the MPL set-up and the relevant wavelength was selected using appropriate bandpass filters. The MPL apparatus consisted of a 10X

expansion telescope that was used to effectively overfill the objective ($60\times$ oil immersion Plan Apochromat, NA = 1.4, Nikon) that focused the laser beam into the resin. The coverslip upon which structures were fabricated was positioned to be facing the objective with the adhesion-promoted side in contact with the resin (i.e. light was focused on the near surface of the sample cell). Fabrication was performed by translating the sample using a computer-controlled 3D positioning stage (MP-285, Sutter Instruments). The incident laser power was controlled using a pair of calcite polarizers. Dosimetry studies were performed by laser writing of free-spanning lines that were written at various incident average laser powers and stage scan speeds. The range of laser powers was chosen to span the range from the threshold power for polymerization to the power at which damage to the sample occurred. For each excitation power, lines were fabricated at four different scan speeds: 60, 40, 20 and 10 $\mu\text{m/sec}$. The scan speed was limited on the high end by the repetition rate of laser used (1 kHz). Both the lateral and axial dimensions of the written lines were determined using scanning electron microscopy (1530, LEO).

The lines were written by scanning the focus of the laser beam between pre-fabricated support structures. Two different types of support structures were utilized. The first type of structure, as illustrated in Fig. 2(a), consisted of parallel rectangular walls (20 μm wide, 30 μm tall, 1 cm long) spaced by gaps that ranged from 2 to 5 μm . Due to the large dimensions of these structures, the 82 MHz repetition rate laser system was used in conjunction with a high-speed precision translation stage (XPS, Newport). These structures were written using the DABSB-triacrylate resin described above. The structures were developed and then backfilled with either the DABSB or DABP-triacrylate resin for line writing. The second type of support structure, shown in Fig. 2(b), was a rectangular “stack of logs” structure (20 μm wide, 15 μm tall, 100 μm long, 5-10 μm spacing). These structures were fabricated in the same resin with the same laser source and excitation wavelength used for the dosimetry studies. Since using the lower repetition rate amplified system (Spitfire) required greater fabrication time, this porous structure was chosen over the more solid structure.

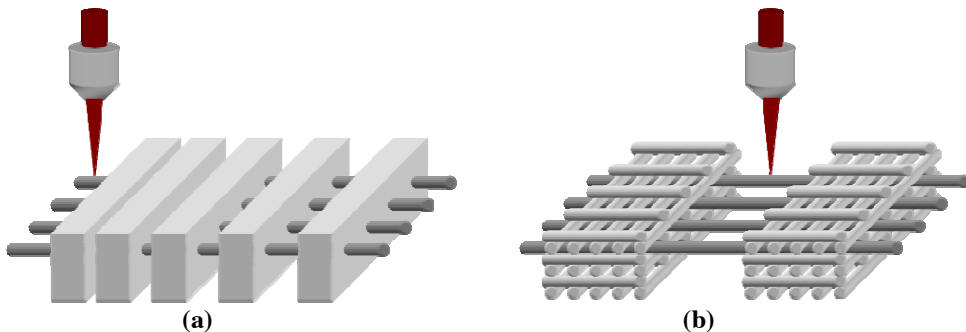


Fig. 2. Schematic illustrations of both types of support structures used for dosimetry studies: (a) rectangular solid walls and (b) rectangular “stack of logs” structure.

2.3 PC fabrication and stop-band characterization

Woodpile-type face-centered tetragonal photonic crystal structures [7] were fabricated using the DABP-triacrylate resin to demonstrate the applicability of short wavelength MPL in the fabrication of free-standing microstructures. Woodpile structures were fabricated with lateral line-to-line spacings of 0.5 μm or 0.85 μm , vertical layer spacings of ~0.34 μm , and a height of 10 unit cell layers, with overall dimensions of 20 $\mu\text{m} \times$ 20 μm . The wavelength-dependent transmission spectra were characterized using a white-light continuum (spectral bandwidth 450 - 1200 nm) that was generated by focusing 2-3 μJ of 1.3 μm excitation from the optical parametric amplifier into a 2 mm calcium fluoride window. This light was focused into the

PC sample and the transmission spectrum was collected using a liquid nitrogen cooled CCD array (LN/CCD-1100-PB, Princeton Instruments) coupled to a spectrograph (SP150, Acton). The PC samples were mounted on a rotation stage and transmission spectra were collected for various angles of incidence.

3. Results and discussion

3.1 Feature sizes and thresholds

Arrays of lines were written between supports, as discussed above, at various powers and scan speeds in order to establish both the threshold for multiphoton writing of polymeric lines and the minimum feature sizes that could be obtained reliably with laser wavelengths of 730 and 520 nm for the resin systems examined. In order to provide statistically meaningful data to support this analysis, between three and six lines have been analyzed for a given power and scan speed. Furthermore, multiple measurements have been performed on any given line (made possible by their considerable lengths) thereby increasing the number of data points for analysis. The threshold power has been defined as the lowest average laser power at which the line survival probability (ratio of the number of lines that survived the developing or rinsing process to the total number of lines written) is more than 80%. This definition provides not only a statistical metric for the threshold power but also makes physical sense for the fabrication of reliable structures. Survival probabilities are expected to decrease at lower powers due to the reduction of feature size as well as crosslinking density both of which result in reduced mechanical strength of the polymerized structure. For this reason, the choice of support structure employed can have an effect on the threshold power. This will be addressed below.

A representative set of fabricated lines for each resin system is shown in Fig. 3. These sets of lines were written at their respective threshold powers at a scan speed of 60 $\mu\text{m/sec}$. Figure 3(a) depicts lines written in the DABSB-triacrylate resin at 730 nm with a threshold power of about 0.9 μW (the power quoted is that at the sample). The resulting lines exhibit diameters of $200 \pm 15 \text{ nm}$. This sub-diffraction limited resolution (the diffraction limited spot-size should be about 320 nm) is typical for MPL and results from the superlinear dependence of multiphoton absorption (MPA) on intensity coupled with the thresholding nature of the polymerization process [10]. This same resin system has been investigated for MPL at 730 nm [6] using a similar optical layout but employing the same Ti:Sapphire oscillator system described above. The feature resolution determined at threshold using this laser oscillator system is consistent with the findings discussed in this work using the amplified laser system. Furthermore, when taking into account the dependence of the absorbed excitation dose on repetition rate and pulsedwidth, the average laser powers at threshold found using each source are also consistent with one another. However, the aspect ratios of the polymerized structures determined in the two works are somewhat different. Individual voxels fabricated by MPL are known to take the shape of ellipsoids of revolution where the height in the axial direction is greater than the widths in the lateral directions. This aspect ratio was determined to be roughly 3:1 using the high repetition rate laser system [6] whereas a ratio of 5:1 was found in this work for the amplified kHz laser. Given the significantly larger peak powers used with the amplified system compared to the oscillator system (nearly 300 times greater), it is possible that the unusually high aspect ratios found here are due to self-focusing and self-trapping effects that can lead to polymerization beyond the typical Rayleigh range [17].

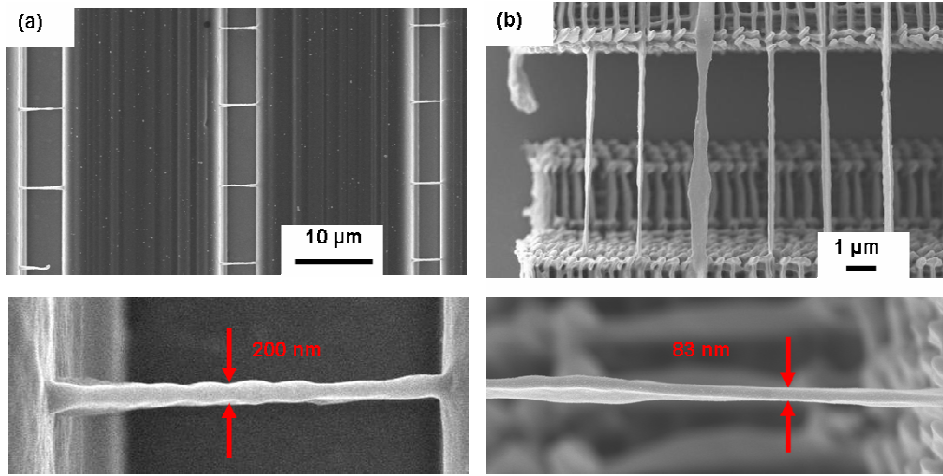


Fig. 3. SEM overview images of lines fabricated at threshold powers with (a) 730 nm excitation using DABSB-triacrylate resin and with (b) 520 nm excitation using DABP-triacrylate resin. Aerial views of support structures described in Fig. 2 are clearly visible in each image. Magnified images of a single line are shown below their respective overview images.

Figure 3(b) shows lines written at 520 nm using the DABP-containing resin system. At the determined threshold power of about $0.7 \mu\text{W}$ (at the sample), the diameters of the resulting written lines are $80 \pm 5 \text{ nm}$. A number of observations can be made regarding MPL using the DABP-triacrylate resin. Firstly, as for the DABSB system, sub-diffraction-limited features are observed (the diffraction-limited spot-size is $\sim 225 \text{ nm}$ for 520 nm excitation). However, the roughly 2.4 times reduction in feature size compared to structures fabricated with 730 nm excitation illustrates that the resolution is fundamentally tied to the wavelength of the excitation. It should be noted that although dispersion of the refractive index of the resin system results in a slightly larger refractive index at 514.5 nm (1.496) compared to 730 nm (1.485), the effect on the resulting numerical aperture (and consequently the focal spot size) is negligible. Secondly, not only are these feature sizes some of the smallest to be written by MPL, but the mechanical stability of these free-spanning lines are evident by their high survival probability despite the large length-to-width ratios of the lines (nearly 100 to 1). Thirdly, the DABP initiator system exhibited a comparable power threshold to that of the DABSB system which itself has been shown to outperform a number of commercially available photoinitiators when used for two-photon microfabrication [6]. Finally, the voxel aspect ratio (of height to width) was found to be 7:1. While self-focusing or self-trapping effects may again play a role here it is not clear why the ratio is higher than that of the DABSB system. However, this may be due to a linear dispersion effect resulting in a higher index change upon polymerization at 520 nm or a nonlinear dispersion effect that gives rise to a larger nonlinear refractive index at 520 nm. This large aspect ratio is evident in Fig. 3(b) where the lines have experienced some torsional forces, most likely during development, leading to some twisting of the lines. This torsion should be ameliorated for support structures providing smaller gaps (smaller length-to-width line ratios), and threshold powers should also decrease for such support structures. This will be elaborated on below.

3.2 Dosimetry and order of multiphoton absorption process

The results of the dose-dependent photo-induced polymerization study for the DABSB-triacrylate resin system are shown in Fig. 4. Figure 4(a) plots line widths (or diameters)

versus inverse scan speed (proportional to exposure or dwell time) for a number of different excitation powers. Clearly, line widths initially grow larger and then approach a constant value with increasing dwell time for a given power. The features also grow larger for increasing power at a particular inverse scan speed. The minimum feature size of 200 nm and the threshold power of 0.90 μW are clearly evident in the graph. Assuming that a written voxel can be described as an ellipsoid of revolution with equivalent widths in both lateral directions (given by the data in Fig. 4(a)) and a height dictated by the 5:1 aspect ratio described above, the voxel volume versus dwell time (or inverse scan speed) can be plotted. This is shown in Fig. 4(b).

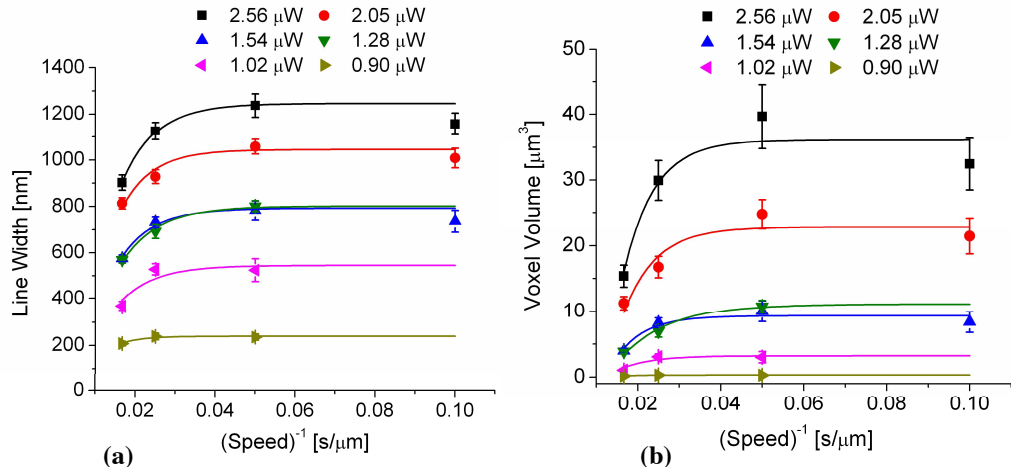


Fig. 4. Dosimetry studies on lines fabricated with 730 nm excitation using DABSB-triacrylate resin. Measured (a) line widths and (b) calculated voxel volumes (see text) as a function of inverse scan speed for different excitation powers. Error bars are given by standard deviations of experimentally measured line widths. The solid lines in (a) are guides for the eye whereas in (b) they represent fittings according to Eq. (1) as described in the text.

The data in Fig. 4(b) can be fitted to the following equation [6],

$$V = A[1 - \exp(-B \cdot t)] \quad (1)$$

where V is the volume of the polymerized voxel, t is the exposure time (proportional to the inverse scan speed) and A and B are fitting parameters. The polymer growth rate is then given by the product of these two parameters, i.e. $R_p = A \cdot B$. The growth rates determined from the fitting curves in Fig. 4(b) are plotted versus the corresponding average laser power in Fig. 5. It has been shown that the rate of polymer growth is proportional to $(I)^{N/2}$ [18] where I is the intensity of the laser source (linearly proportional to the average laser power) and N is the order of the MPA process involved in the polymerization process. Therefore, by fitting the data in Fig. 5 to a power law function of the form

$$R_p = C \cdot |P - P_{th}|^{N/2}, \quad (2)$$

where C is a constant, P is the average power, and P_{th} is the threshold power, the order of the MPA process can be determined. The fit to the data in Fig. 5 reveals a power law dependence of $N \approx 3.1$ suggesting that an effective three-photon process correctly describes the MPA process involved in the photoinduced polymerization. Thus, while it is clear that the DABSB chromophore exhibits a strong two-photon resonance at 730 nm, absorption of at least one

additional photon is involved in the photoinitiation process. As such, the process can be thought of as a 2PA event followed by one-photon absorption, or a 2+1 MPA event. It should be noted that the determination of the order of this process may be affected by non-local effects such as diffusion, which have not been taken into account in this analysis. The threshold power is identified as $0.66 \mu\text{W}$ by the fitting curve in Fig. 5. The discrepancy between this value of P_{th} and the value of $0.90 \mu\text{W}$ found in the dosimetry studies discussed above stems from the influence of the developing process. A larger threshold power ensures greater crosslinking of the polymer resulting in the requisite survival probability.

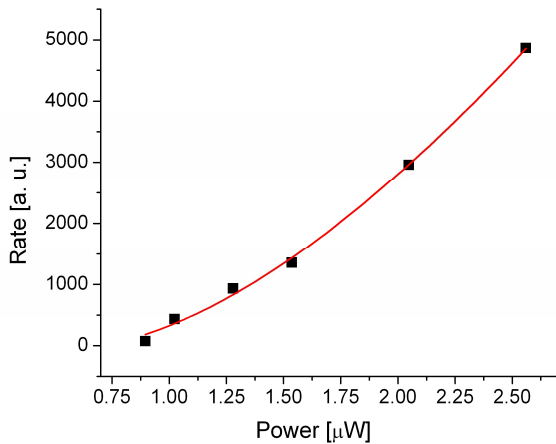


Fig. 5. Polymer growth rates (as determined in text) derived from the dosimetry studies shown in Fig. 4(b) as a function of excitation power. The experimentally determined values are given as filled black squares and the red solid line indicates a fitting according to Eq. 2. The fitting parameters are: $C = 1770$, $P_{\text{th}} = 0.66$, and $N = 3.14$.

Figure 6 shows the dosimetry results for the DABP-triacrylate resin system. Once again, the trends of the line widths as a function of dwell time and the power are consistent with the results found for the DABS-triacrylate resin system described above. Furthermore, a threshold power of $0.70 \mu\text{W}$ along with the corresponding 80 nm minimum feature size is also evident in the graph. However, a reliable study of the polymerization kinetics, similar to the one performed above for the DABS-triacrylate resin, was not possible due to the larger errors associated with these line width measurements. This was mainly attributed to the smallness of the feature sizes and their tight grouping (the difference between the smallest and largest feature size measured was a mere 35 nm , as opposed to nearly 1000 nm for the DABS data using 730 nm excitation). More detailed work on these polymerization kinetics studies will be conducted in the future using a more stable source of visible wavelength, high repetition rate, femtosecond pulse excitation to accurately determine the order of the MPA process involved.

3.3 PC structures and stop-band spectra

Using the DABP-triacrylate resin system, woodpile-type face-centered tetragonal PC structures were fabricated. Compared to the previous lines fabricated between supporting

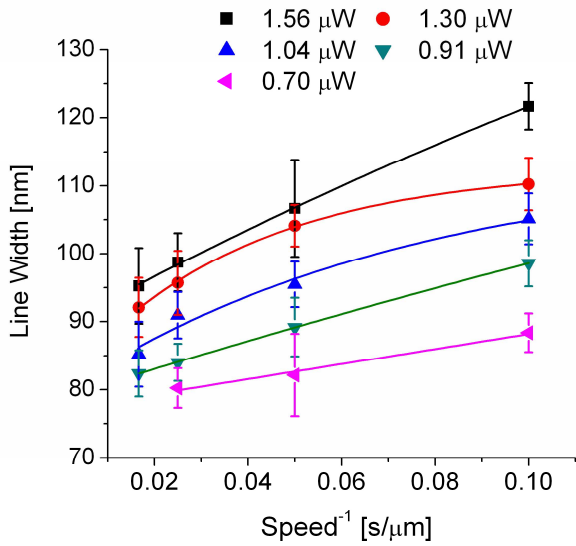


Fig. 6. Dosimetry studies on lines fabricated with 520 nm excitation using the DABP-triacrylate resin. Error bars are given by standard deviations of experimentally measured line widths. The solid lines are guides for the eye.

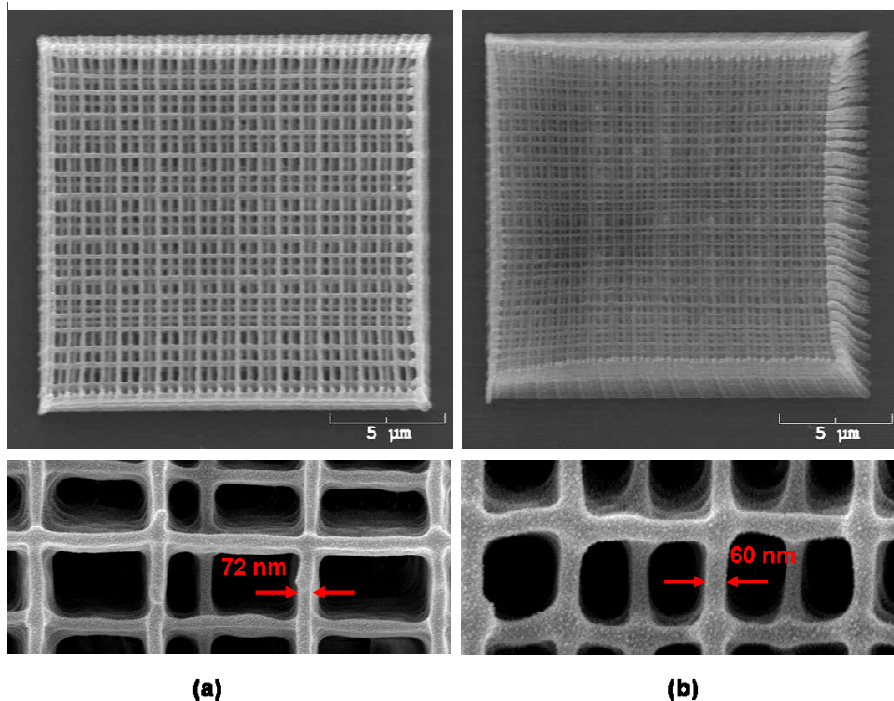


Fig. 7. SEM overview images of woodpile-type PC structures fabricated with 520 nm excitation at (a) 0.60 μW and at (b) 0.45 μW using the DABP-triacrylate resin. Fabrication parameters of PCs were: lateral line-to-line spacings of (a) 0.85 μm and (b) 0.5 μm , axial layer-to-layer spacings of $\sim 0.34 \mu\text{m}$, and scan speeds of 60 $\mu\text{m/sec}$. Magnified images of the PC structures are shown below their respective overview images.

walls separated by 5-10 μm , these PC structures provide smaller separation between anchoring points and therefore more structural support for the lines written by MPL. Consequently, since these structures enhance the survival probability of the line features, even smaller features than the 80 nm diameter lines reported above have been achieved in these structures. Figure 7 shows two typical PC structures written at 520 nm with the DABP-triacrylate resin. In all, three sets of PCs were fabricated with powers of 0.75, 0.60 and 0.45 μW at a scan speed of 60 $\mu\text{m/sec}$ with lateral spacings of either 0.50 μm or 0.85 μm . Average widths of the measured lines were 81 ± 7 nm, 75 ± 5 nm, and 63 ± 5 nm, respectively. It is immediately apparent that this more mechanically supportive structure lowers the threshold power for polymerization and thereby allows for finer resolution structures to survive.

Transmission spectra for several of the PC structures described above were collected according to the procedures detailed in Section 2.3. The spectra for different angles of incidence for one of these structures are shown in Fig. 8. Fringes are observed at longer wavelengths (> 900 nm) and the period corresponds to a film thickness of ~ 14 μm consistent with the height of the PC structure. Stop bands have been observed and are indicated by arrows and appear at 717 nm, 810 nm, 890 nm, and 986 nm for incident angles of 0, 10, 20, and 30 degrees, respectively. This trend of the red-shifting of PBG stop bands with increasing angle of incidence has been observed previously [19]. It is apparent that the ability to fabricate PBGs with high-resolution mechanically stable lines permits the design of structures possessing fundamental stop bands in the short-wavelength portion of the near-infrared spectral region. In fact, the spectral position of the stop band is primarily dictated by the axial layer-to-layer spacing of the PBG. The large aspect ratio of the lines written at 520 nm using the DABP-triacrylate resin gave rise to large line heights (~ 0.34 μm) and therefore placed a lower limit on the axial spacing that could be achieved with these PBGs. Stop bands in the visible portion of the spectrum could, therefore, be achieved by reducing this line height resulting in smaller axial layer-to-layer spacings. The contrast in the observed stop bands can be enhanced by improving the fidelity of the fabricated PBG structures and by utilizing higher index materials.

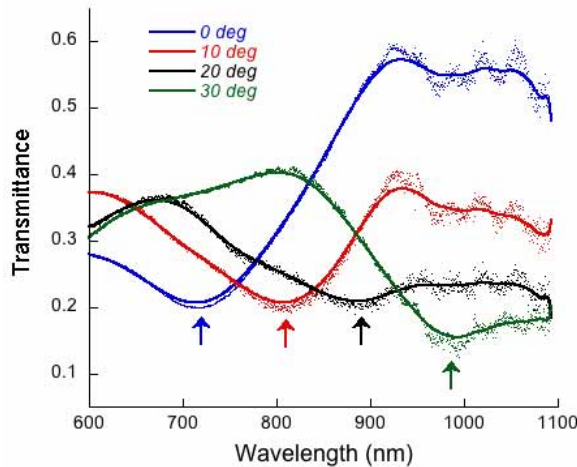


Fig. 8. Transmission spectra of PBG structure fabricated with 520 nm excitation at 0.60 μW using the DABP-triacrylate resin. The dotted lines indicate experimentally observed spectra while the solid lines are merely guides for the eye. Observed stop bands have been indicated by appropriately colored arrows. Fabrication parameters of PBG were: average line width of 75 nm, lateral line-to-line spacing of 0.5 μm , axial layer-to-layer spacing of ~ 0.34 μm , scan speed of 60 $\mu\text{m/sec}$.

4. Conclusion

The use of laser-induced polymerization using a photoinitiator with a sizable two-photon absorption cross-section in the visible wavelength region (520 nm) has allowed for multiphoton 3D lithography with nanoscale lateral feature resolution: line widths of 80 nm for long, free-spanning lines and 65 nm line widths in woodpile photonic crystal structures. Comparative studies with two-photon absorbing initiators at 730 and 520 nm show that the minimum lateral feature sizes are below the diffraction limit for the resin systems examined at both excitation wavelengths, while the height to width aspect ratio for the features written with high intensity pulses at a 1kHz repetition rate is two to three times greater than typically observed for writing with high repetition rate sources. The fabrication of nanoscale lines via visible wavelength MPL has been utilized to fabricate initial polymeric photonic crystal structures with lateral periods of 500 nm, which gave stop bands in the near infrared spectral region. The capability for reliable formation of nanoscale features using MPL should have a substantial impact on the fabrication of photonic, electronic and MEMS devices, among others.

Acknowledgments

Support of this work by the Office of Naval Research APEX Consortium (N00014-05-0303) and the National Science Foundation, through the Science and Technology Center for Materials and Devices for Information Technology Research (DMR-0120967), is gratefully acknowledged. We wish to thank Dr. Mariacristina Rumi for providing preliminary two-photon absorption data on the DABP photoinitiator compound. We also thank Greg Walker for a sample of the DABSB compound.